COMMUNICATIONS

Measurement of Relaxation Rates of N^H and H^α Backbone Protons in Proteins with Tailored Initial Conditions

Oscar Millet,* Elisabetta Chiarparin,† Philippe Pelupessy,† Miquel Pons,*,1 and Geoffrey Bodenhausen†,‡,2

*Departament de Química Orgànica, Universitat de Barcelona, Martí i Franquès 1-11, 08028 Barcelona, Spain; †Section de chimie, Université de Lausanne, BCH, 1015 Lausanne, Switzerland; and ‡Département de chimie, associé au CNRS, Ecole Normale Supérieure, 24 rue Lhomond, 75231 Paris Cedex 05, France

Several methods are presented for the selective determination of spin–lattice and spin–spin relaxation rates of backbone protons in labeled proteins. The relaxation rates of amide protons in ^{15}N labeled proteins can be measured by using two-way selective cross-polarization (SCP). The measurement of H^α relaxation rates can be achieved by combining this method with homonuclear Hartmann–Hahn transfer using doubly selective irradiation. Various schemes for selective or nonselective inversion of the longitudinal proton magnetization lead to different initial recovery rates. The methods have been applied to lysine K6 in ^{15}N-labeled human ubiquitin and to leucine L5 in ^{15}N- and ^{13}C-labeled octapeptide YG*G*F*LRRI (GFL) in which the marked residues are ^{15}N- and ^{13}C-labeled. © 1999 Academic Press

Dynamic processes in peptides and proteins can be characterized by measuring relaxation rates of ^{15}N nuclei (1, 2), of proton-carrying ^{13}C nuclei (3), and of carbonyl ^{13}C nuclei (4). So far, relaxation rates of ^{1}H nuclei have not been exploited as much as those of ^{15}N and ^{13}C, despite the development of selective homonuclear magnetization transfer methods which make it possible to measure proton relaxation parameters in proteins (5, 6). Because proton relaxation often obeys multi-exponential laws, the decay and recovery curves may be difficult to interpret. Moreover, homonuclear scalar couplings between protons lead to modulations of spin-echoes. Nevertheless, the initial rate approximation can usually provide reasonable estimates of self- and cross-relaxation rates (7–10). Longitudinal proton relaxation rates have been determined in ^{15}N-labeled proteins (11, 12). Structural changes in peptides and proteins can be inferred from line-broadening of proton signals (13) and proton relaxation measurements allow identification of dimeric domains in proteins (14). In paramagnetic proteins (11, 15, 16) the proton relaxation rates are enhanced in the vicinity of paramagnetic centers (17). Analysis of nitrogen relaxation in terms of spectral densities requires the determination of the auto-relaxation rate of the proton directly attached to the nitrogen (18).

In this Communication, we describe several one-dimensional methods to measure the transverse and longitudinal relaxation rates of selected protons. These methods are particularly suitable when only a small number of protons in strategic positions need to be characterized. The methods use two-way selective cross-polarization (SCP) (19, 20). The magnetization of a chosen proton is transferred to a heteronucleus and back again (e.g., ^{1}H → ^{15}N → ^{1}H) by applying two radiofrequency (RF) fields at the chemical shifts of the two nuclei. Provided the amplitudes of the continuous-wave RF fields are very weak (e.g., about half the magnitude of the relevant heteronuclear scalar coupling), the effect of RF field inhomogeneities becomes negligible (19). Such experiments are more efficient than selective heteronuclear correlation techniques obtained by inserting selective pulses into HSQC-type experiments. The longitudinal or transverse relaxation rates of selected protons can be measured in the usual fashion by using inversion-recovery or Carr–Purcell–Meiboom–Gill (CPMG) methods prior to selective cross-polarization. Water suppression can be achieved by applying gradients while the longitudinal magnetization resides on the ^{15}N, without recourse to any selective proton pulses, thus avoiding saturation effects and signal attenuation.

Figure 1a shows the selective detection scheme that has been used to measure longitudinal and transverse relaxation rates of individual amide protons in ^{15}N-labeled proteins or peptides. Figure 2 shows the recovery of the longitudinal magnetization of the amide proton of lysine K6 in ubiquitin following a nonselective inversion pulse. It is strongly affected by cross-relaxation with neighboring protons. The Solomon equation describing the time-dependence of the longitudinal magnetization of a chosen proton I_i interacting with N other protons I_j and with a heteronuclear spin S_k is given by

$$d\Delta I_{iz}(t)/dt$$

$$= -\rho_i \Delta I_{iz}(t) - \Sigma_{j \neq i}^{N} \sigma_{ij} \Delta I_{jz}(t) - \sigma_{ik} \Delta S_{kz}(t), \quad [1a]$$
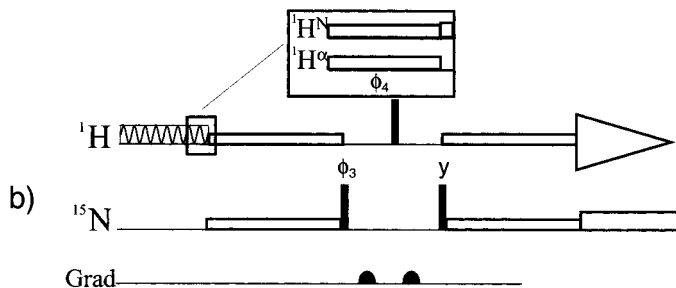
---

1 E-mail: miquel@guille.qo.ub.es. Fax: 34 93 3397878.

2 To whom correspondence should be addressed. E-mail: Geoffrey.Bodenhausen@ens.fr. Fax: 33 1 44 32 33 97.

DETECTION

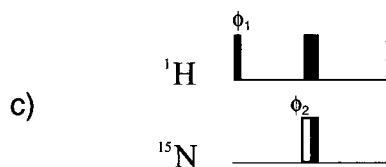### Selective Detection of Amide Protons
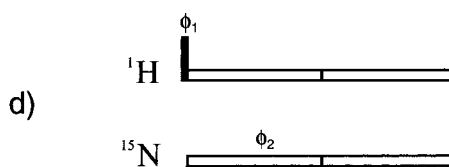

a)
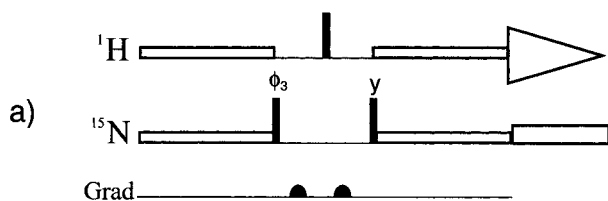
Selective Detection of Alpha Protons

b)

PREPARATION

Semi-selective Inversion with BIRD module

c)

Selective Inversion with two-way SCP

d)

FIG. 1. Modules for sequences for the determination of longitudinal and transverse relaxation rates of H^N and H^α protons in peptides and proteins. (a) Selective detection of $I_x(H^N)$ and (b) selective detection of $I_x(H^\alpha)$ in ^{15}N labeled macromolecules. Extended horizontal rectangles correspond to low-amplitude spin-locking pulses for heteronuclear cross-polarization transfer and for ^{15}N decoupling. Between the two cross-polarization steps, the ^{15}N magnetization is stored along the z axis, while the magnetization of the I spins (including solvent magnetization) is destroyed by a $\pi/2$ pulse, sandwiched between two gradient pulses that spoil the transverse magnetization. The cosinusoidally modulated rectangle in (b) corresponds to a doubly selective irradiation (DSI) that leads to a transfer of magnetization between H^α and H^N. (c) Semi-selective inversion of all $I_z(H^N)$ using a BIRD pulse sequence (the narrow open rectangle represents a $\pi/2$ pulse that is alternated in phase). (d) Selective inversion of a chosen $I_z(H^N)$ with two selective cross-polarization (SCP) steps. The phase-cycling is common for all the sequences: $\phi_1 = y, -y, y, -y, y, -y, y, -y$; $\phi_2 = x, x, -x, -x, x, x, -x, -x$; $\phi_3 = y, y, y, y, -y, -y, -y, -y$; $\phi_{receiver} = x, -x, -x, x, -x, x, x, -x$. If sequence (b) is used, $\phi_4 = x$ in the first 8 scans and $\phi_4 = -x$ in the next 8 scans, while the receiver phase is reversed between the first and second series of 8 scans.

where ρ_i is the self-relaxation rate, σ_{ij} and σ_{ik} are the homo- and heteronuclear cross-relaxation rates; $\Delta I_{iz}(t) = I_{iz}(t) - I_{iz}^{eq}$, $\Delta I_{jz}(t) = I_{jz}(t) - I_{jz}^{eq}$, and $\Delta S_{kz}(t) = S_{kz}(t) - S_{kz}^{eq}$, where I_{iz}^{eq}, I_{jz}^{eq}, and S_{kz}^{eq} are the expectation values of the I_{iz}, I_{jz}, and S_{kz} operators in equilibrium. Effects of cross-correlation between fluctuating interactions are neglected. The initial rate of recovery is determined not only by the inversion of I_i through $\Delta I_{iz}(t = 0)$, but also by the initial conditions $\Delta I_{jz}(t = 0)$ of all protons in the vicinity and by $\Delta S_{kz}(t = 0)$. Provided one does *not* apply any pulses to the neighboring protons I_j and to the S_k spins, Eq. [1a] can be simplified since $\Delta I_{jz}(t = 0) = \Delta S_{kz}(t = 0) = 0$.

To compare the various experiments presented in this Communication, it is convenient to record inversion-recovery data in the manner of "difference spectroscopy." If one considers inversion-recovery spectra such as in Fig. 2, the corresponding difference spectra of Fig. 3 can be obtained simply by subtracting the equilibrium magnetization. Thus, Eq. [1a] must be considered twice with two different sets of initial conditions: $\Delta I_{iz}^A(t = 0)$, $\Delta I_{iz}^B(t = 0)$, $\Delta I_{jz}^A(t = 0)$, $\Delta I_{jz}^B(t = 0)$, $\Delta S_{kz}^A(t = 0)$, and $\Delta S_{kz}^B(t = 0)$, where experiment A refers either to selective, semiselective, or nonselective inversion, while the initial populations are usually

not perturbed in experiment B. This amounts to observing the return to the demagnetized state, rather than to thermal equilibrium. Equation [1a] must be replaced by

$$d[I_{iz}^A(t) - I_{iz}^B(t)]/dt = -\rho_i[I_{iz}^A(t) - I_{iz}^B(t)]$$
$$- \Sigma_{j \neq i}^N \sigma_{ij}[I_{jz}^A(t) - I_{jz}^B(t)]$$
$$- \sigma_{ik}[S_{kz}^A(t) - S_{kz}^B(t)]. \qquad [1b]$$

The initial rate is determined by the conditions immediately after the preparation period:

$$\lim_{t \to 0} d[I_{iz}^A(t) - I_{iz}^B(t)]/dt = -\rho_i[I_{iz}^A(0) - I_{iz}^B(0)]$$
$$- \Sigma_{j \neq i}^N \sigma_{ij}[I_{jz}^A(0) - I_{jz}^B(0)]$$
$$- \sigma_{ik}[S_{kz}^A(0) - S_{kz}^B(0)]. \qquad [2]$$

If the components $I_{jz}(0)$ and $S_{kz}(0)$ are prepared in the same way (e.g., inverted or left unperturbed) in the two experiments
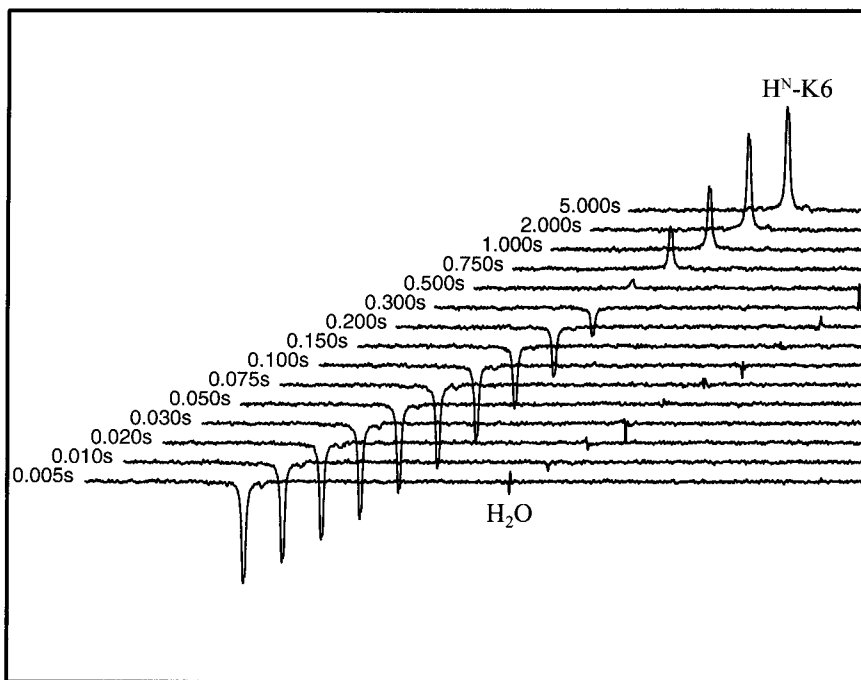
FIG. 2. Combination of nonselective inversion recovery with selective observation of H^N of lysine K6 (4.1 ppm downfield from the water resonance) in a 1.5 mM sample of ^{15}N-labeled human ubiquitin (in H_2O/D_2O 9:1). For all experiments 128 scans were accumulated at 303 K and 300 MHz, using the sequence of Fig. 1a preceded by a nonselective proton π pulse and recovery intervals ranging from 5 ms to 5 s. The spin-locking fields are set to about 40 Hz with a duration of 11 ms.

A and B, the initial values $[I_{jz}^A(0) - I_{jz}^B(0)]$ and $[S_{kz}^A(0) - S_{kz}^B(0)]$ vanish.

In macromolecules such as ubiquitin ($\tau_c \approx 4$ ns at 300 K), the number N of neighboring protons can be very large, so that different inversion schemes have a strong influence on the initial recovery rates (Table 1). On the other hand, in a small peptide such as GFL the cross-relaxation rates are smaller than the self-relaxation rates and the density of protons is lower than in ubiquitin, so that the initial recovery is not strongly affected by the

selectivity of the initial inversion. One can set up suitable initial conditions in view of separating cross- and self-relaxation rates. For H^N amide protons in proteins and peptides, an important contribution to the initial recovery rate stems from the cross-relaxation rate σ_{ij} between H_i^N and the neighboring H_j^α proton. This contribution can be easily removed if only the amide protons are inverted with a sequence for "bilinear rotation decoupling" (BIRD) (21). To obtain difference spectra one may alternate the phase of one of the adjacent $\pi/2$ pulses applied to ^{15}N in the BIRD
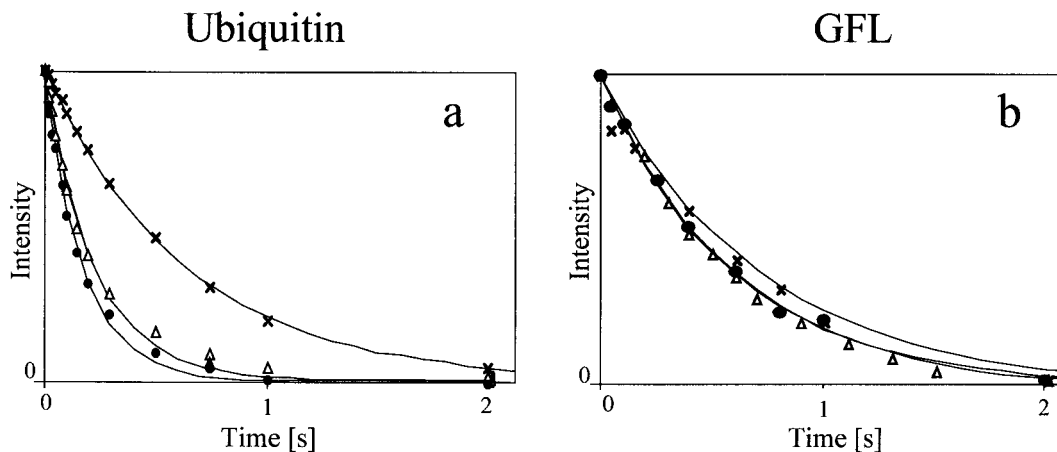
FIG. 3. Inversion recovery curves obtained in the manner of difference spectroscopy with different inversion schemes (a) for the H^N proton of lysine K6 in ubiquitin and (b) for the H^N proton of leucine L5 in GFL peptide (YGGFLRRI). (x) Nonselective π pulse; ($\triangle$) BIRD inversion as in Fig. 1c; ($\bullet$) two-way SCP as in Fig. 1d. The initial recovery rates derived from the curves are given in Table 1.

TABLE 1
Initial Rates of Recovery Measured
with Different Inversion Methods

Inversion scheme	N^H of lysine K6 in ubiquitin[a] (s^{-1})	N^H of leucine L5 in GFL[b] (s^{-1})
Nonselective π	1.55 (1.50–1.60)[c]	1.33 (1.20–1.46)[c]
BIRD module of Fig. 1c	4.68 (4.26–5.10)	1.60 (1.53–1.67)
Scheme of Fig. 1d	5.64 (5.08–6.20)	1.65 (1.50–1.80)

[a] At 300 MHz and 303 K in H_2O/D_2O 9:1.
[b] GFL = TGGFLRRI, measured at 500 MHz and 300 K in D6-DMSO.
[c] Numbers in brackets give estimated confidence limits.

sequence in Fig. 1c. Note that it is not possible to subtract the equilibrium magnetization in this case because of transverse relaxation during the BIRD sequence. One also has to pay attention to cross-relaxation between H^N and the attached ^{15}N nucleus. The effect of heteronuclear cross-relaxation (which is proportional to $\sigma_{ik}\Delta S_{kz}$) is equivalent to homonuclear cross-relaxation (proportional to $\sigma_{ij}\Delta I_{jz}$) between two protons separated by about 3, 5, or 7 Å for $\tau_c = 1, 4$, or 12 ns at 400 MHz. The effect of the attached ^{15}N nucleus can be averaged out by alternating the phase Φ_1 of the first proton $\pi/2$ pulse in the BIRD sequence in both experiments A and B. This changes the relative sign of $I_{iz}(t = 0)$ with respect to $S_{kz}(t = 0)$ just after the BIRD sequence. Measurements on H^N of lysine K6 in ubiquitin and of leucine L5 in GFL (YGGFLRRI) are shown in Fig. 3. The initial recovery rates measured with BIRD and with a nonselective inversion are given in Table 1 along with estimated confidence limits. The rates were obtained by Levenberg–Marquardt nonlinear fitting of the recovery curves. The relaxation of the amide proton is slower after nonselective inversion than after semiselective inversion. Indeed, after nonselective inversion the first two terms on the right-hand side of Eq. [2] contribute. In both GFL and ubiquitin the cross-relaxation rates σ_{ij} are negative ($\tau_c > 1/\omega_0$) so that the second term of Eq. [2]

partly cancels the first term, ρ_i and $\Sigma\sigma_{ij}$ having opposite signs. Therefore, the BIRD inversion of the H^N nuclei, which allows one to remove the effect of the second term in Eq. [2], leads to an acceleration of the decay of the H^N magnetization. Inversion of the H^N magnetization by a BIRD sequence leaves the aromatic protons unaffected, hence Eq. [2] becomes

$$\lim_{t \to 0} d[I_{iz}^A(t) - I_{iz}^B(t)]/dt = -\rho_i[I_{iz}^A(0) - I_{iz}^B(0)]$$

$$-\sum_{j \neq i}^{amides} \sigma_{ij}[I_{jz}^A(0) - I_{jz}^B(0)]. \quad [3]$$

The contributions to the initial recovery rate of a selected H^N proton stemming from cross-relaxation to other amide protons are often not negligible. Such contributions can be removed by selectively inverting only the amide proton under investigation. This can be achieved by using two selective heteronuclear cross-polarization steps as shown in Fig. 1d. It is possible, as in the BIRD sequence of Fig. 1c, to observe the return to the demagnetized state by phase-alternating one of the spin-locking pulses applied to the nitrogen-15 channel, while alternating the receiver phase. Cross-relaxation pathways involving other protons are eliminated, since both experiments A and B are identical from the point of view of protons that are not filtered through the selected nitrogen-15 nucleus. The effects of heteronuclear cross-relaxation can be cancelled by alternating the phase Φ_1 of the first proton $\pi/2$ pulse in Fig. 1d. Thus, for each of the two experiments A and B (which differ in the phase $\Phi_2 = \pm x$ of the first selective pulse applied to ^{15}N), one must alternate the phase $\Phi_1 = \pm y$ of the first proton pulse, while alternating the receiver phase. With reference to Eq. [2], it is apparent that the experiment of Fig. 1d causes the last two terms to vanish completely so that neither σ_{ij} nor σ_{ik} affect the initial recovery. The initial recovery rates obtained with the scheme of Fig. 1d (see Table 1) are the fastest in the series, thus proving that cross-relaxation is largely suppressed.

When the selective detection scheme of Fig. 1a follows a Carr–
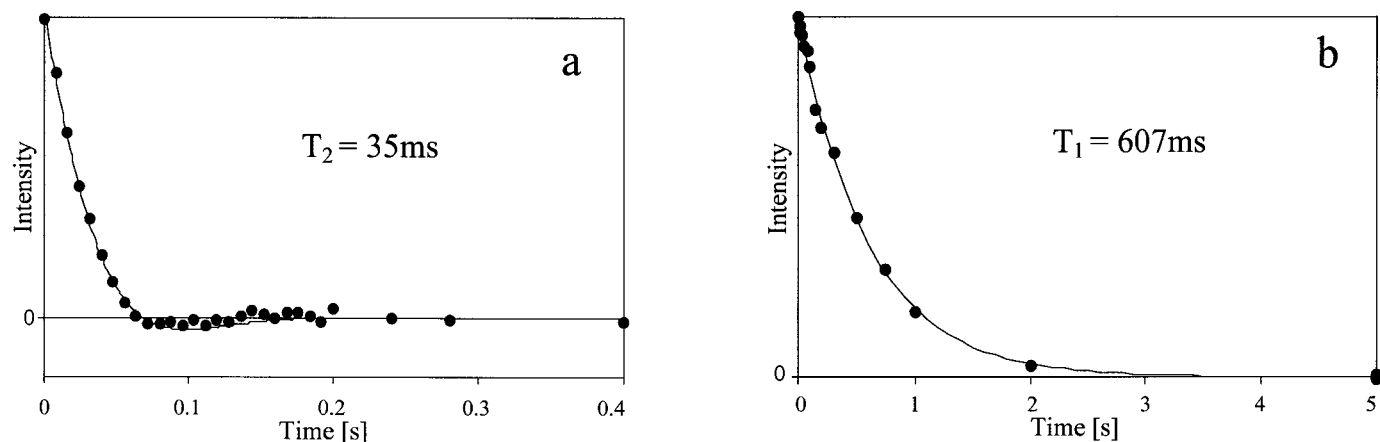
FIG. 4. (a) Transverse relaxation measurement of H^N in Lysine K6 of ubiquitin, recorded using a CPMG-module with intervals of 4 ms between the proton π pulses. The curve is fitted with $\exp(-t/T_2)\cos(\pi Jt)$ (where both T_2 and J are adjusted) in order to take into account the homonuclear scalar coupling $^3J(H^\alpha H^N)$, found to have a magnitude of 7.1 Hz. (b) Longitudinal relaxation after nonselective inversion of H^α in Lysine K6, detected with the module of Fig. 1b.

Purcell–Meiboom–Gill spin–echo sequence (*22*), it is possible to measure transverse relaxation rates of selected protons. The echo decay for H^N of lysine K6 in ubiquitin is shown in Fig. 4a.

All experiments can be adapted to observe H^α protons in ^{15}N-labeled proteins, as shown in Fig. 1b. The $I_x(H^\alpha)$ magnetization can be transformed into $I_x(H^N)$ through the scalar coupling $^3J(H^\alpha H^N)$ using a homonuclear Hartmann–Hahn transfer using doubly selective irradiation (DSI) (*5, 6, 23*). For the sake of illustration, we have combined this detection scheme with nonselective inversion recovery. Figure 4b shows a nonselective T_1 measurement of H^α in K6 in ubiquitin.

The experiments presented in this work allow one to measure longitudinal and transverse relaxation times of chosen H^N and H^α protons in ^{15}N-labeled peptides and proteins. These methods allow one to separate different contributions to longitudinal relaxation. The one-dimensional experiments are time-efficient and easy to implement. They are particularly suitable when only a few protons in strategic positions need to be investigated.

Experiments on ubiquitin (obtained from VLI research, 1.5 mM, $H_2O:D_2O$ 9:1, pH 4.5) were performed with a Bruker DRX-300 spectrometer equipped with an inverse detection double resonance probe, while experiments with the octapeptide GFL (TGGFLRRI, enriched in 6 sites: TG[^{15}N,^{13}C]G[^{15}N,^{13}C]F[^{15}N,^{13}C]LRRI, 1 mM in D_6-DMSO, Cambridge Isotope Laboratories Inc.) were carried out on a Bruker DMX-500 spectrometer with an inverse detection TBI triple resonance probe. The temperature was set to 300 K for GFL and to 303 K for ubiquitin.

REFERENCES

1. A. G. Palmer, R. A. Hochstrasser, D. P. Millar, M. Rance, and P. E. Wright, Characterization of amino acid side chain dynamics in a zinc finger peptide using ^{13}C-NMR spectroscopy and time resolved fluorescence spectroscopy. *J. Am. Chem. Soc.* **115**, 6333–6345 (1993).

2. L. E. Kay, D. R. Muhandiram, N. A. Farrow, Y. Aubin, and J. D. Forman-Kay, Correlation between dynamics and high affinity binding in an SH2 domain interaction, *Biochem.* **35**, 361–368 (1996).

3. N. Nirmala and G. Wagner, Measurement of ^{13}C relaxation times in proteins by two-dimensional heteronuclear ^1H–^{13}C correlation spectroscopy, *J. Am. Chem. Soc.* **110**, 7557–7558 (1998).

4. K. T. Dayie and G. Wagner, Carbonyl carbon probe of local mobility in ^{13}C, ^{15}N-enriched proteins using high-resolution nuclear magnetic resonance, *J. Am. Chem. Soc.* **119**, 7797–7806 (1997).

5. B. Boulat, R. Konrat, I. Burghardt, and G. Bodenhausen, Measurement of relaxation rates in crowded NMR spectra by selective coherence transfer, *J. Am. Chem. Soc.* **114**, 5412–5414 (1992).

6. B. Boulat and G. Bodenhausen, Measurement of proton relaxation rates in proteins, *J. Biomol. NMR* **3**, 335–348 (1993).

7. R. L. Vold and R. R. Vold, Transverse relaxation in heteronuclear coupled spin systems: AX, AX_2, AX_3 and AXY, *J. Chem. Phys.* **64**, 320–322 (1976).

8. R. L. Vold and R. L. Vold, Nuclear magnetic relaxation in coupled spin systems, *Prog. Nucl. Magn. Reson. Spectrosc.* **12**, 79–131 (1978).

9. L. G. Werbelow and D. M. Grant, Intramolecular dipolar relaxation in multispin systems, *Adv. Magn. Reson.* **9**, 189–299 (1977).

10. J. Kowalewski, Nuclear spin relaxation in diamagnetic fluids. Part 1. General aspects and inorganic applications, *Ann. Rep. NMR Spectrosc.* **22**, 308–414 (1990).

11. I. Bertini, M. M. J. Couture, A. Donaire, L. D. Eltis, I. C. Felli, C. Luchinat, M. Piccioli, and A. Rosato, The solution structure refinement of the paramagnetic reduced high-potential iron–sulfur protein I from *ectothiorhodospira halophila* by using stable labelling and nuclear relaxation, *Eur. J. Biochem.* **241**, 440–452 (1996).

12. J. R. Gillespie and D. Shortle, Characterization of long-range structure in the denatured state of staphylococcal nuclease I. Paramagnetic relaxation enhancement by nitroxide spin labels, *J. Mol. Biol.* **268**, 158–169 (1997).

13. G. S. Shaw, R. S. Hodges, and B. D. Sykes, Calcium induced peptide association to form an intact protein domain. ^1H-NMR structural evidence, *Science* **249**, 280–283 (1990).

14. D. Yang, Y. Yamamoto, E. Kanaya, S. Kanaya, and K. Nagayama, Characterization of an artificial dimer of ribonuclease H using ^1H-NMR spectroscopy, *J. Biomol NMR* **7**, 29–34 (1996).

15. J. G. Huber, J. Moulis, and J. Gaillard, Use of ^1H longitudinal relaxation times in the solution structure of paramagnetic proteins. Application to 4Fe–4S proteins, *Biochem.* **35**, 12705–12711 (1996).

16. A. Donaire, Z. Zhou, M. W. W. Adams, and G. N. La Mar, ^1H-NMR investigation of the secondary structure, tertiary contacts and cluster environment of the four ion ferredoxin from the hyperthermophilic archaedon thermococcus litoralis, *J. Biomol. NMR* **7**, 35–47 (1997).

17. K. Clark, L. B. Dugad, R. G. Bartsch, M. A. Cusanovich, and G. N. La Mar, An interpretative basis of the proton NMR hyperfine shifts for structure determination of high-spin ferric hemoproteins. Implications for the reversible thermal unfolding of ferricytochrome c' from *rhodopseudomonas palustris, J. Am Chem. Soc.* **118**, 4654–4664 (1996).

18. Peng G. and Wagner G., Mapping of spectral density functions using heteronuclear NMR relaxation measurements, *J. Mag. Res.* **98**, 308–332 (1992).

19. E. Chiarparin, P. Pelupessy, and G. Bodenhausen, Selective cross polarization in solution state NMR, *Mol. Phys.* **95**, 759–767 (1998).

20. P. Pelupessy, E. Chiarparin, and G. Bodenhausen, Excitation of selected proton signals in NMR of isotopically labeled macromolecules, *J. Magn. Reson.* **138**, 178–181.

21. G. R. Garbow, D. P. Weitekamp, and A. Pines, Bilinear rotation decoupling of homonuclear scalar interactions, *Chem. Phys. Lett.* **93**, 504–508 (1982).

22. R. Freeman and H. D. W. Hill, in "Dynamic Nuclear Magnetic Resonance Spectroscopy" (L. M. Jackman and F. A. Cotton, Eds.), Academic Press, New York (1975).

23. C. Zwahlen, S. J. F. Vincent, and G. Bodenhausen, *in* "Proceedings of the International School of Physics Enrico Fermi, 'Double Resonance'" (B. Maraviglia, Ed.), pp. 397–412, North-Holland, Amsterdam (1993).